

On the Approximate Calculation of Half-Power Beam Width for Uniform Circular Arrays

Hua Tang*, Xianzheng Zong*, and Zaiping Nie

School of Electronic Science and Engineering
University of Electronic Science and Technology of China (UESTC), Chengdu, Sichuan 610054, P.R.C.
tungh@foxmail.com

Abstract — In this paper, the approximate calculations of the half-power beam width (HPBW) of a uniform circular array (UCA) in azimuth and elevation are investigated by numerical calculations and data analysis methodology. Two corresponding formulas are proposed to approximately estimate the HPBW of UCA in azimuth and elevation under different pointing directions of the main lobe. The proposed formulas' validities are examined by comparing the results with the ones directly calculated from the array factor. Besides, the accuracies of the proposed approximate formulas are evaluated in both absolute error and error rate. The calculation speed is assessed in time as well. Numerical simulation results are provided to show the proposed formulas' performances.

Index Terms — Approximate calculation, estimation formulas, half-power beam width (HPBW), uniform circular array (UCA).

I. INTRODUCTION

Uniform circular arrays (UCAs), also known as uniform ring array, have some special characteristics compared with uniform linear arrays (ULAs) and uniform planar arrays (URAs). It can be known from the antenna theory that UCAs can provide a 2-dimension (2D) angular scan, namely angular scan in azimuth and elevation. Moreover, UCAs can scan in azimuth plane from 0° to 360° almost without distortion for the radiation pattern, since the mutual coupling effect is the same for each element. The applications of UCAs hence can be found in many fields, such as source localization [1], the direction of arrival (DoA) estimation [2], wireless communications [3], smart antennas [4], and so on.

Lots of studies have been reported on UCAs. The authors in [5] investigate the DoA estimation via moving a UCA in predefined path under multipath environments. 2D DoA estimations are studied for UCAs [6-8]. The phase-mode-decomposition-based and optimization-based methods are investigated to suppress the side lobe of UCA [9]. The effect of mutual coupling is studied for UCA from the electromagnetic aspect [10]. Only a few of researches pay attention to the fast calculation of

UCA's HPBW which is very complicated to compute from the definition. Though the calculation of HPBW for UCA is investigated in [11], it is only available for the main lobe pointing at the azimuth plane and still very complicated. A simple formula with only two parameters, wavelength and array radius, is proposed to estimate the HPBW of UCA roughly [12, 13], yet it is only applicable under the zenith angle of main beam being 90° .

It is necessary to figure out an easy and quick solution on calculating the HPBW of UCA, because fast HPBW estimation is an important and meaningful job in the pre-design of UCA. For example, before designing an UCA for 2D DoA estimation application, the HPBW of the UCA's main lobe needs a quick and rough evaluation. Estimating the HPBW of UCA is an energy-consuming and time-consuming task due to no formula with a simple form like that of the one for ULA [14].

Accordingly, the study of this paper focuses on finding out a simple method to estimate the HPBW for UCA. Based on numerical computation and data analysis, a formula is proposed to approximately calculate the azimuth HPBW for UCA under different zenith angles of the main lobe. Compared to the formula in [12, 13] which only can calculate the azimuth HPBW under the zenith angle of 90° , the proposed formula is more applicable. Considering the situation that the two main beams, which are symmetric about the azimuth plane (xy -plane in Fig. 1), of the UCA can be identified definitely, a formula with simple form is also proposed to estimate the elevation HPBW roughly. The proposed formulas not only can estimate the HPBW of UCA correctly, but also achieve the good calculation accuracy, especially for azimuth HPBW. More importantly, the proposed formulas far surpass the definition method in calculation speed.

The remainder of this paper is organized as follows. Section II describes the general geometry of UCA. The approximate estimations of HPBWs in azimuth and elevation are investigated in Section III where two corresponding estimation formulas are also proposed. The proposed formulas' performances in validity,

accuracy and speed are studied via numerical simulations in Section IV. Finally, conclusions are drawn in Section V.

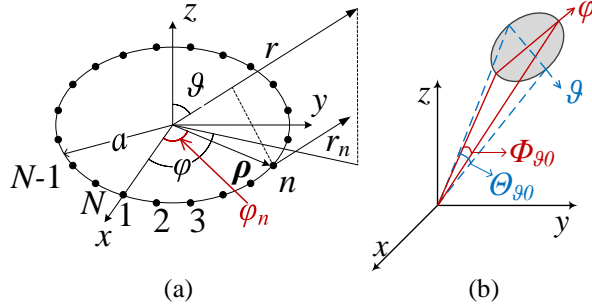


Fig. 1. (a) Configuration of UCA with N -element, and (b) definition of HPBW in azimuth and elevation.

II. GEOMETRY OF UCA

A configuration of UCA with N elements located in xy -plane is illustrated in Fig. 1 (a) [15]. The array radius is a , and the n th element is located at the phase angle of φ_n where $n=1, 2, \dots, N$. Each element has an associated weight I_n and phase α_n , meaning the amplitude and phase of excitation current. The array factor (AF) can be written as [14, 15]:

$$AF(\varphi, \vartheta) = \sum_{n=1}^N I_n e^{j(ka \sin(\vartheta) \cos(\varphi - \varphi_n) + \alpha_n)}, \quad (1)$$

$$\alpha_n = -ka \sin(\vartheta_0) \cos(\varphi_0 - \varphi_n),$$

where k , φ , ϑ are the wavenumber, azimuth angle, zenith angle, respectively, φ_n is the angular location in azimuth plane and given by:

$$\varphi_n = 2\pi \frac{n-1}{N}. \quad (2)$$

The element spacing of the UCA can be obtained as:

$$d = \frac{2\pi}{N} a. \quad (3)$$

Letting $d = \lambda/2$ and substituting it into (3), we have:

$$\frac{a}{\lambda} = \frac{N}{4\pi}. \quad (4)$$

The left term of (4) is usually named electrical length. Equation (4) reveals the proportional relationship between the electrical length of array radius and the number of array elements.

III. ANALYSIS OF THE APPROXIMATE CALCULATION OF HPBW

In order to define the HPBW for UCA clearly, the HPBWs in azimuth and elevation, Φ_{ϑ_0} and θ_{ϑ_0} , are used to describe the HPBW of UCA under the zenith angle of ϑ_0 , illustrated in Fig. 1 (b). Letting $\varphi = \varphi_0$ and $\vartheta = \vartheta_0$ in the AF in (1), we have:

$$AF(\varphi) = \sum_{n=1}^N I_n e^{j(ka \sin(\vartheta_0) \cos(\varphi - \varphi_n) + \alpha_n)}, \quad (5)$$

$$\alpha_n = -ka \sin(\vartheta_0) \cos(\varphi_0 - \varphi_n),$$

and

$$AF(\vartheta) = \sum_{n=1}^N I_n e^{j(ka \sin(\vartheta) \cos(\varphi_0 - \varphi_n) + \alpha_n)}, \quad (6)$$

$$\alpha_n = -ka \sin(\vartheta_0) \cos(\varphi_0 - \varphi_n).$$

In order to attain the common results, we assume

that the isotropic radiators are employed as the elements of the UCA in this paper. Considering a UCA model with uniform excitation amplitude, I_n in (5) and (6) can be set to 1, and the HPBWs in azimuth and elevation can be directly computed via (5) and (6) respectively at the half-power points. Although computing the HPBWs from (5) and (6) is the most accurate approach, it is obviously a tough job.

The azimuth HPBW of UCA under $d = \lambda/2$ can be approximately calculated by [12, 13]:

$$\Phi \approx 21^\circ \cdot \frac{\lambda}{a}. \quad (7)$$

However, (7) only can be used to calculate the azimuth HPBW under $\vartheta = 90^\circ$, namely (7) is not available under $\vartheta \neq 90^\circ$. It is also demonstrated in Table 1.

Table 1: Azimuth HPBW under different ϑ_0

ϑ_0 (deg.)	Φ_{ϑ_0} (deg.)	$\Phi_{\vartheta_0}/\Phi_{90}$
10	49.948	5.803
20	25.210	2.929
30	17.226	2.001
40	13.394	1.556
50	11.237	1.306
60	9.939	1.155
70	9.160	1.064
80	8.740	1.015
90	8.607	1.000

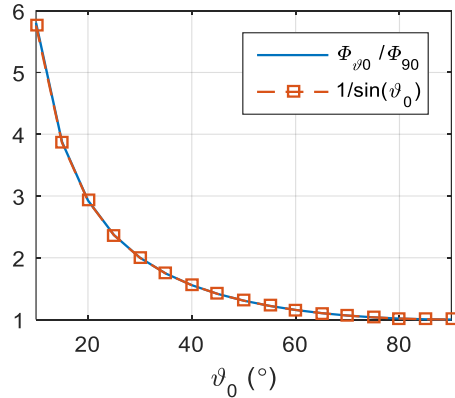


Fig. 2. Trend of Φ_{ϑ_0} normalized by Φ_{90} .

According to (5), we can find that both components of the main lobe direction, azimuth angle and zenith angle, are contained in the AF besides the electrical length of array radius. It implies that the azimuth HPBW should be affected by the direction of the main lobe. According to the knowledge of array antenna, it is known that the azimuth HPBW remains unchanging with the azimuth angle of the main lobe. It suggests that the azimuth HPBW must have a relationship with the zenith angle. Based on (5), it is easy and reasonable to deduce that Φ_{ϑ_0} has a relationship with the sine or cosine of the

zenith angle. To further investigate the relationship, the azimuth HPBWs of UCA are directly calculated from (5) under different values of ϑ_0 , and recorded in Table 1.

In Table 1, the zenith angles and the corresponding azimuth HPBWs, namely ϑ_0 and Φ_{ϑ_0} , are depicted on the first and second columns in degree respectively, and the ratios of the azimuth HPBWs corresponding to different ϑ_0 to azimuth HPBW under $\vartheta_0 = 90^\circ$, i.e., Φ_{90} , are presented on the third column. The data on the second and third columns indicate that the azimuth HPBW decreases with the increasing of ϑ_0 until $\vartheta_0 = 90^\circ$. In addition, the results of $\Phi_{\vartheta_0}/\Phi_{90}$ show a minimum ratio of 1 at $\vartheta_0 = 90^\circ$. It is easy to know that the property is coincident with that of $1/\sin(\vartheta_0)$. To observe the trend of the data clearly, the ratio of $\Phi_{\vartheta_0}/\Phi_{90}$ and $1/\sin(\vartheta_0)$ are plotted in Fig. 2. It can be seen that the curve of $\Phi_{\vartheta_0}/\Phi_{90}$ highly agrees with that of $1/\sin(\vartheta_0)$.

Therefore, the azimuth HPBW of UCA can be summarized as:

$$\Phi_{\vartheta_0} \approx \Phi_{90} \times \frac{1}{\sin(\vartheta_0)}, \quad (8)$$

where Φ_{90} is the HPBW under $\vartheta_0 = 90^\circ$ and given by (7). Substituting (7) into (8), an estimation formula for the azimuth HPBW of a UCA can be obtained as:

$$\Phi_{\vartheta_0} \approx 21^\circ \cdot \frac{\lambda}{a \sin(\vartheta_0)}, \quad (9)$$

where $\vartheta_0 \in (0^\circ, 180^\circ)$. Note that the absolute value of Φ_{ϑ_0} in (9) is approaching to infinity when ϑ_0 is closing to 0° and 180° . This apparently do not happen in reality. Under such situation, it is meaningless to consider the azimuth HPBW. Consequently, to avoid the two singular points and ensure the validity of (9), the value of ϑ_0 is limited in $(10^\circ, 170^\circ)$.

According to the antenna theory, the variation of elevation HPBW is too complicated to be described by a simple function for $\vartheta_0 \in (0^\circ, 180^\circ)$, since the array has two symmetric main beams with respect to the plane the array located in and the beams cannot be definitely separated when the element number is too small or the value of ϑ_0 is close to 90° . To estimate the elevation HPBW in a simple way, we only consider the situation that the two main beams of a UCA can be separated definitely. Thus, only $\vartheta_0 \in (10^\circ, 70^\circ) \cup (110^\circ, 170^\circ)$ are considered in the elevation HPBW's investigation in this paper.

Similarly, the elevation HPBWs under different values of ϑ_0 are computed via (6), as recorded in Table 2. The data on the second and third columns show that with the growing of ϑ_0 , the elevation HPBWs, θ_{ϑ_0} , increase gradually, as well as the normalized θ_{ϑ_0} . According to the AF in (6), the elevation HPBW must have a connection with the sine or cosine of ϑ_0 . It is easily to deduce that the elevation HPBW is related to $1/\cos(\vartheta_0)$. To observe the variations more clearly, the normalized θ_{ϑ_0} and $1/\cos(\vartheta_0)$ are plotted in Fig. 3.

Table 2: Elevation HPBW under different of ϑ_0

ϑ_0 (deg.)	θ_{ϑ_0} (deg.)	Normalized θ_{ϑ_0}
10	2.622	0.341
20	2.748	0.358
30	2.982	0.388
40	3.371	0.439
50	4.021	0.523
60	5.181	0.674
70	7.685	1.000

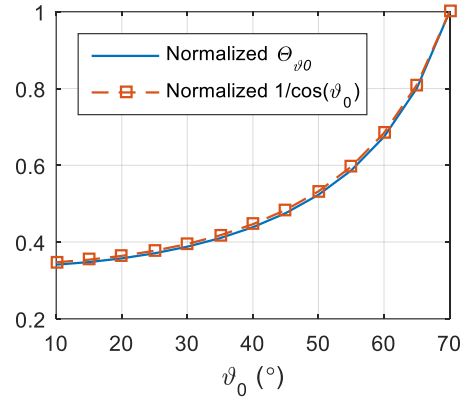


Fig. 3. Trend of the normalized θ_{ϑ_0} .

Based on the results in Table 2 and Fig. 3, the approximate formula for estimating the elevation HPBW of a UCA can be summarized as below:

$$\theta_{\vartheta_0} \approx 21^\circ \cdot \frac{\lambda}{a \cos(\vartheta_0)}, \quad (10)$$

where $\vartheta_0 \in (10^\circ, 70^\circ)$ and $\vartheta_0 \in (110^\circ, 170^\circ)$.

The proposed formulas, (9) and (10), depict the simple relations that the azimuth HPBW of UCA is inversely proportional to the sine of zenith angle of the main lobe and the electrical length of array radius, and the elevation HPBW is inversely proportional to the cosine of zenith angle of the main lobe and the electrical length of array radius. The overall computational costs of (5) and (6) are given by $O(N)$, while those of the proposed approximate formulas only require $O(1)$. Apparently, the computational complexities of (5) and (6) that increase with the growing of n are higher than those of the proposed approximate formulas, especially for a large UCA.

IV. RESULTS

In this section, the validities and accuracies of the proposed formulas are studied in numerical simulations as well as the calculation speed in time. Since the results validities and accuracies are symmetric about $\vartheta_0 = 90^\circ$, for the sake of brevity, only those for $\vartheta_0 \leq 90^\circ$ are provided in this paper.

A. Validity verification

According to proposed formulas, the HPBW of the

UCA in azimuth and elevation are only affected by λ/a and ϑ_0 . To examine the validities, the results of the HPBW obtained from (9) and (10) are compared with those computed via the AF in (5) and (6) under different values of λ/a and ϑ_0 respectively. As aforementioned, the study of paper focuses on the uniform tapering case. Accordingly, we can set $I_n = 1$ in (5) and (6).

The verification of (9) under different values of ϑ_0 is provided in Fig. 4 where the curves labeled “via (5)” and “via (9)” represent the results obtained by (5) and (9) respectively. Two array radii examples, $a = 3.18\lambda$ and $a = 4.77\lambda$, are presented in this simulation. It can be seen that the results obtained from the proposed formula (9) are highly in agreement with those computed by the AF in (5) under different zenith angles. It suggests that the proposed approximate formula (9) can not only get correct results, but also be applicable under different zenith angles of the main lobe for UCA. In addition, it also suggests that the proposed approximate formula is suitable for different array radii.

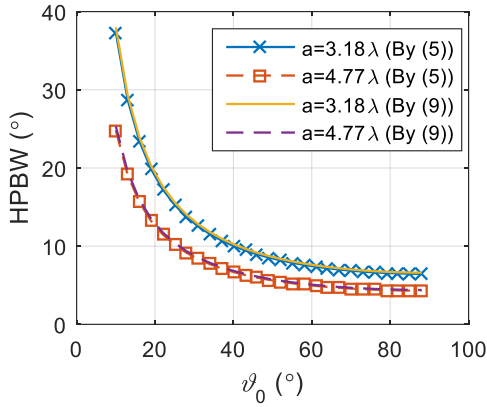


Fig. 4. Azimuth HPBWs under different zenith angles.

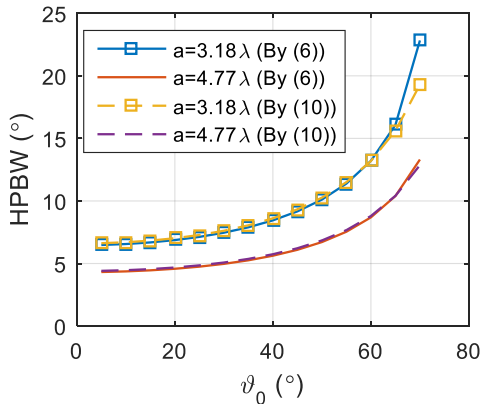


Fig. 5. Elevation HPBWs under different zenith angles.

The elevation HPBWs under different zenith angles for $a = 3.18\lambda$ and $a = 4.77\lambda$ are presented in Fig. 5. It can be seen that the results computed from (10) agree

with the ones calculated by (6) well, especially for $a = 4.77\lambda$. The results also indicate that (10) can obtain a correct elevation HPBW with an acceptable error, if the two main beams of a UCA can be definitely identified. Besides, the proposed estimation formula (10) is not only suitable for different zenith angles of the main lobe, but also applicable under different array radii.

Therefore, the proposed approximate formulas, (9) and (10), can be used to estimate the HPBWs of UCA in azimuth and elevation under different array radii and zenith angles of the main lobe.

B. Calculation error

Since the proposed formulas attain approximate results, the calculation error is a very important characteristic, which directly affects the accuracy of the results and leads to a limitation for the formulas' application. Consequently, the accuracies of the proposed formulas should be evaluated.

To investigate the accuracy of the proposed approximate formula (9), taking the results computed by (5) as a reference, the azimuth HPBWs of UCA are calculated by (9) under different zenith angles and array radii. The comparisons are presented in both absolute error and error rate, as depicted in Fig. 6 and Fig. 7.

It is clear from the results in Fig. 6 that the differences between the results calculated by (5) and (9) are very small. The absolute errors decrease with the growing of ϑ_0 , and reach the minimums at $\vartheta_0 = 90^\circ$. Besides, the errors decline with the growing of array radii in general, though the decreased calculation errors are smaller and smaller with the array radius growing. Moreover, the trends of the calculation errors for different array radii are almost the same, which implies the good agreements of the calculation errors under different array radii.

Figure 7 shows the contrary trends that the maximum error rates occur at $\vartheta_0 = 90^\circ$, and the error rates grow as ϑ_0 increases till 90° . The results also show that the maximum calculation error rates under different radii are almost the same, and their upper limits are around 2.2% at $\vartheta = 90^\circ$. In addition, as the array radius grows, the error rates decline slower and slower and tend to stay steady at the maximums when ϑ_0 is approaching to 90° . It means that the growing of array radius weakens the influence of the elevation component of the main lobe's direction to the calculation error rate. Both absolute error and error rate in Fig. 6 and Fig. 7 reflect that the proposed approximate formula (9) gets a good accuracy.

The accuracy of the proposed estimation formula (10) for the elevation HPBW is also evaluated in absolute error and error rate, as depicted in Fig. 8 and Fig. 9. It can be seen from Fig. 8 that the calculation errors are very small, except for the case of $a = 3.18\lambda$ under $\vartheta_0 > 65^\circ$. The calculation errors gradually increase as ϑ_0 is approaching to 90° , especially for the small array radius

cases, since it is harder and harder to distinguish the two main beams of the UCA. Generally, the calculation errors remain unchanging till $\vartheta_0 = 50^\circ$, and then begin to decline and bound. The results indicate that with the increasing of array radii, the calculation errors decrease and the values of ϑ_0 at bounding points increase.

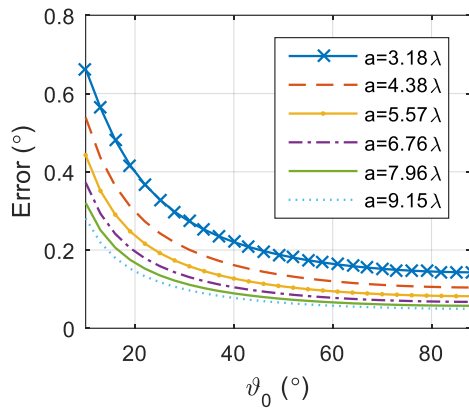


Fig. 6. Absolute error of (9).

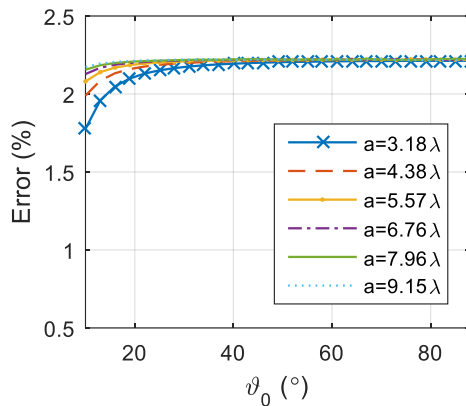


Fig. 7. Error rate of (9).

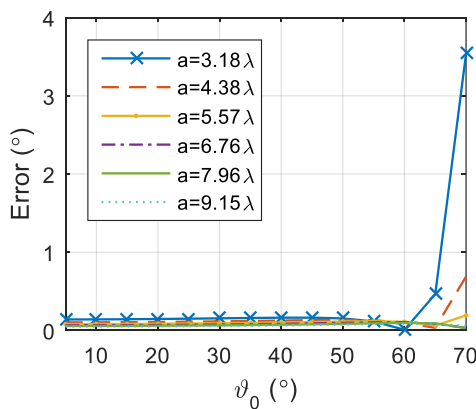


Fig. 8. Absolute error of (10).

The simulation results in Fig. 9 show that the error rates begin with around 2.2%, and with the growing of

ϑ_0 , they decrease gradually. The error rates bound at a certain ϑ_0 which grows as the array radius increases. The reason of the error rates grows quickly when $\vartheta_0 > 65^\circ$ for the case of $a = 3.18\lambda$ is mentioned before. In general, the larger the array radius is, the steadier the error rates are. Meanwhile, the general trends of error rate are coincident with those of the absolute errors in Fig. 8.

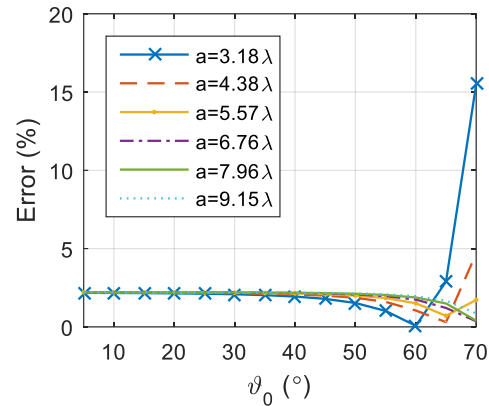


Fig. 9. Error rate of (10).

C. Calculation speed

To further show the proposed formulas' advantage, the computational speeds are evaluated based on the calculation time. Due to the same calculation speed of (5) and (6) and the same calculation speed of (9) and (10), for the sake of brevity, only the calculation times of (5) and (9) are presented. The results based on 10,000 iterations are depicted in Fig. 10. It shows that the calculation time of (9) remains constant even if N increases, yet the computational time of (5) grows with the increasing of N . Moreover, the calculation time of (9) is at least 2,000 times less than that of (5) in this example, and this ratio grows with the increasing of N . It implies that the proposed formulas can approximately estimate the HPBW of a UCA at a very high speed, compared with the involuted and time-consuming conventional method, i.e., by (5) and (6).

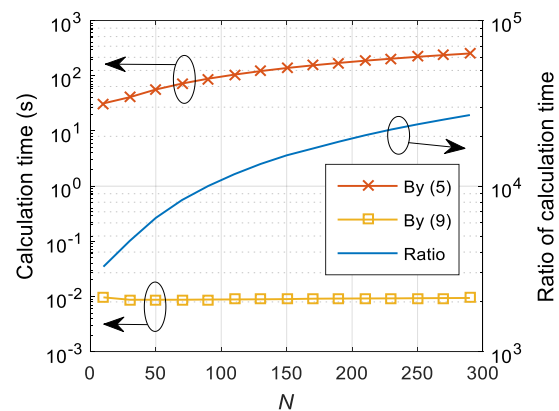


Fig. 10. Calculation times based on 10,000 iterations.

V. CONCLUSION

In this paper, two very simple formulas are proposed to estimate the HPBW of UCA in azimuth and elevation roughly under different main lobe directions. In contrast with computing the HPBW directly from definition, the proposed approximate formulas provide an easy and fast approach to estimate the HPBW of UCA in azimuth and elevation. The proposed formula for azimuth HPBW can get not only a correct result but also a good accuracy with a maximum error rate of 2.2%. The formula for elevation HPBW also can estimate the elevation HPBW correctly with an acceptable accuracy. Moreover, the proposed formulas attain an extremely high calculation speed. Therefore, the study in this paper provides a simple and quick method to estimate the HPBW of UCA.

REFERENCES

- [1] Y. Wu, H. Wang, Y. Zhang, and Y. Wang, "Multiple near-field source localization with uniform circular array," *IET Electronics Letters*, vol. 49, no. 24, pp. 1509-1510, Nov. 2013.
- [2] J. J. Fuchs, "On the application of the global matched filter to DOA estimation with uniform circular arrays," *IEEE Transactions on Signal Processing*, vol. 49, no. 4, pp. 702-709, Apr. 2001.
- [3] P. Wang, Y. Li, and B. Vucetic, "Millimeter wave communications with symmetric uniform circular antenna arrays," *IEEE Communications Letters*, vol. 18, no. 8, pp. 1307-1310, Aug. 2014.
- [4] P. Ioannides and C. A. Balanis, "Uniform circular arrays for smart antennas," *IEEE Antennas and Propagation Magazine*, vol. 47, no. 4, pp. 192-206, Aug. 2005.
- [5] V. L. Do, T. B. Nguyen, V. K. Dao, and C. H. Nguyen, "Direction finding in multipath environments using moving uniform circular arrays," *2017 3rd International Conference on Frontiers of Signal Processing (ICFSP)*, Paris, pp. 50-54, 2017.
- [6] X. Lian and J. Zhou, "2-D DOA Estimation for Uniform Circular Arrays with PM," *2006 7th International Symposium on Antennas, Propagation & EM Theory*, Guilin, pp. 1-4, 2006.
- [7] Y. Wu and H. C. So, "Simple and accurate two-dimensional angle estimation for a single source with uniform circular array," *IEEE Antennas and Wireless Propagation Letters*, vol. 7, pp. 78-80, 2008.
- [8] B. Liao, Y. T. Wu, and S. C. Chan, "A generalized algorithm for fast two-dimensional angle estimation of a single source with uniform circular arrays," *IEEE Antennas and Wireless Propagation Letters*, vol. 11, pp. 984-986, 2012.
- [9] F. Belfiori, S. Monni, W. Van Rossum, and P. Hoogeboom, "Side-lobe suppression techniques for a uniform circular array," *The 7th European Radar Conference*, Paris, pp. 113-116, 2010.
- [10] W. Jeon, J. H. Kim, and S. Y. Chung, "Effect of mutual coupling on uniform circular arrays with vector antenna elements," *IEEE Antennas and Wireless Propagation Letters*, vol. 16, pp. 1703-1706, 2017.
- [11] J. H. Kim, W. Jeon, and S. Y. Chung, "Asymptotic analysis on directivity and beamwidth of uniform circular array," *IEEE Antennas and Wireless Propagation Letters*, vol. 16, pp. 3092-3095, 2017.
- [12] H. G. Urban, *Handbook of Underwater Acoustic Engineering*. STN, Atlas Elektronik, 2002.
- [13] X. Lurton, *An Introduction to Underwater Acoustics: Principles and Applications*. Springer Science & Business Media, Berlin, 2002.
- [14] C. A. Balanis, *Antenna Theory Analysis and Design*. 3rd ed., John Wiley & Sons, Inc.: New Jersey, USA, 2005.
- [15] F. Gross, *Smart Antennas for Wireless Communications with MATLAB*. McGraw-Hill, New York, 2005.



Hua Tang received the B.S. degree in Electronic Information Engineering from the Southwest University of Science and Technology, Mianyang, China, in 2010. He is currently working towards the Ph.D degree with the School of Electronic Science and Engineering, University of Electronic Science and Technology of China, Chengdu, China. His research interests include antenna selection and signal processing in MIMO and massive MIMO, and antenna theory and technology in mobile communications.



Xianzheng Zong received the B.S., and Ph.D. degrees in Electromagnetic Field and Microwave Technique from the University of Electronic Science and Technology of China (UESTC), Chengdu, in 2002, and 2008, respectively. He was a Lecturer with UESTC, from 2008 to 2011. Since 2011, he has been an Associate Professor with UESTC. His current research interests include antenna theory and technology, computational electromagnetics, and electromagnetic compatibility (EMC).



Zaiping Nie received the B.S. degree in Radio Engineering and the M.S. degree in Electromagnetic Field and Microwave Technology from the University of Electronic Science and Technology of China, Chengdu, China, in 1968 and 1981, respectively.

He is currently a Professor with the Department of Microwave Engineering, UESTC. From 1987 to 1989, he was a Visiting Scholar with the Electromagnetics Laboratory, University of Illinois, Urbana, IL, USA. His current research interests include computational electromagnetics and its applications, antenna theory and techniques, electromagnetic scattering and inverse scattering, and field and waves in inhomogeneous media.